JOURNAL OF CATALYSIS 117, 121–134 (1989)

Steady-State Isotopic Transient-Kinetic Analysis of Iron-Catalyzed Ammonia Synthesis

JOHN U. NWALOR,[1] JAMES G. GOODWIN, JR.,[2] AND PAUL BILOEN†

Chemical and Petroleum Engineering Department, University of Pittsburgh, Pittsburgh, Pennsylvania 15261

Received July 6, 1988; revised October 25, 1988

Steady-state isotopic transient-kinetic analysis of ammonia synthesis catalysis has been conducted over a commercial Fe catalyst (Haldor Topsøe KMIR) permitting, for the first time, *direct* determinations of coverages in reactive intermediates of the working catalyst surface and assessments of the reaction mechanism and surface heterogeneity at steady-state reaction conditions. The reaction was studied in the temperature range 623–773 K, at a total pressure of 204 or 513 kPa, and for a H_2/N_2 ratio of 3. Dinitrogen chemisorption in the absence of H_2 was also measured at 773 K by the transient kinetic technique. The results suggest that *N is the most abundant reactive intermediate. It may be inferred, as expected, that a kinetically significant reaction step exists on the reaction path followed by nitrogen. Hydrogen appears to enhance this step which seems to involve dinitrogen dissociation. The working surface was observed to be heterogeneous with respect to the synthesis reaction. The steady-state isotopic transient curves, at 204 kPa and temperatures of 623 and 673 K, indicate one main pool of nitrogen-containing surface intermediates. At 723 and 773 K, a second less reactive pool of intermediates developed due, perhaps, to the activation of previously dormant or saturated sites or to possible contributions from bulk-phase nitrogen species. Both pools of N-intermediates were kinetically nonuniform. This investigation provides significant new insight into ammonia synthesis catalysis.

INTRODUCTION

The nature and quantity of the species which constitute the main intermediates during heterocatalytic reactions provide important clues to the reaction mechanism and to the nature of the active sites. In view of the dynamic nature of these reactions, any evaluation of the intermediates is best conducted at steady-state working conditions (*1, 2*). It is also essential to be able to distinguish between reactive intermediates on the one hand and "spectator" catalyst-bound species on the other. A goal of the present study was the determination of the abundances of N-containing reactive intermediates during ammonia synthesis over a commercial Fe-based ammonia synthesis catalyst (Haldor Topsøe KMIR) by means of steady-state isotopic transient-kinetic analysis (SSITKA) (*2, 3*) of the reaction. Transient curves which result from such experiments bear relevance to the identification of the important reactive intermediates and to the question of the existence of a single rate-limiting step in ammonia synthesis at practical reaction conditions. It is known that steady-state rate data are alone inadequate for distinguishing between competing mechanistic structures (*4, 5*). The steady-state transient line shapes also contain information on the degree to which the working catalyst surface is kinetically nonuniform.

This study represents the first application of SSITKA to the ammonia synthesis system. In an earlier preliminary study (*6*), unambiguous conclusions could not be made, based on the transient line shapes, about the reaction mechanism. This was due to the employment of a plug-flow type reactor for the reaction system which exhibited product readsorption that was not easily definable (*7*). A gradientless reactor was em-

† Deceased.

[1] Present address: Chemical Engineering Department, University of Lagos, Nigeria.

[2] To whom all correspondence should be addressed.

0021-9517/89 $3.00

ployed for the present study to alleviate such problems.

The SSITKA method, which has hitherto been mainly utilized in the analysis of CO hydrogenation systems (*2, 8–11*), entails abrupt switches in the isotopic composition of the reaction mixture accompanied by the continuous monitoring (by mass spectrometry) of the relaxation and evolution of labeled reactants and products (see Fig. 1). When isotope effects can be neglected, as is the case with the $^{15}N_2$ for $^{14}N_2$ substitution employed in this work, the analysis involves no perturbation of the chemical potential of the reaction ambient.

In order to assess the coverage in H-containing reaction intermediates, isotope switches have to be made between hydrogen and deuterium. Hydrogen for deuterium substitution, however, exhibits isotope effects. In addition, there can be substantial dissolution of hydrogen in stainless-steel reactors such as that employed in this study. This makes H-coverage determination rather imprecise. In spite of these drawbacks, valuable information was obtained about the trajectory of hydrogen (H-path) in the synthesis reaction from hydrogen–deuterium exchange experiments.

EXPERIMENTAL

Reactant Gases

Hydrogen (99.999%) and deuterium (99.99%) were further purified by passage through an activated carbon (Matheson) hydrocarbon trap and a Deoxo (Engelhard)

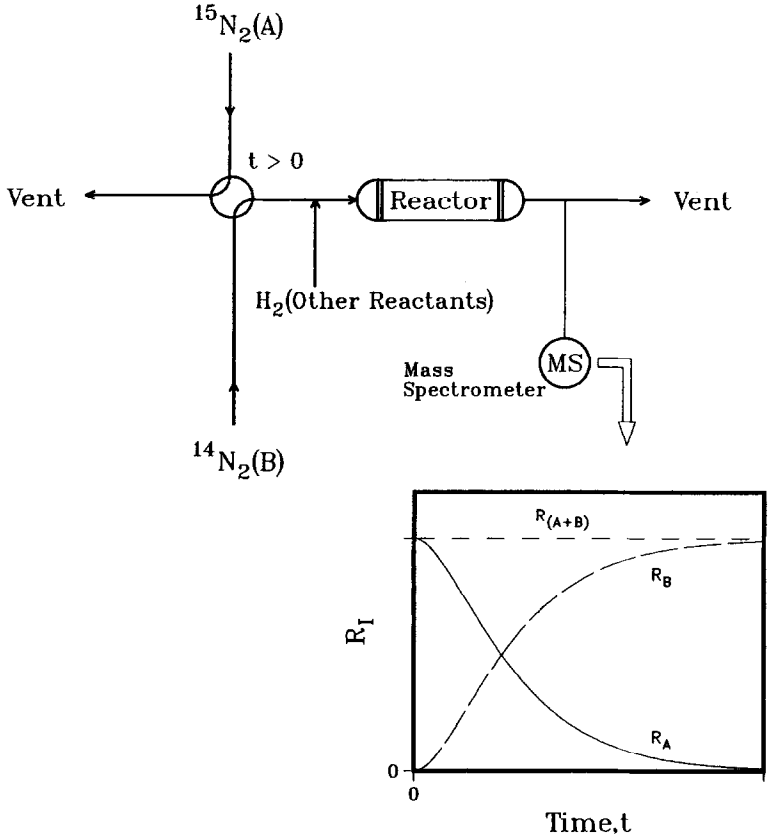

FIG. 1. Schematic of steady-state isotopic transient-kinetic data collection system showing a switch from a reactant isotope, A, to a chemically equivalent isotope, B, and the corresponding typical response curves.

unit followed by a 13X molecular sieve column immersed in liquid nitrogen. He (99.999%) was further purified by a purification train of an activated carbon trap and a liquid nitrogen-cooled 13X molecular sieve column. Normal nitrogen (Linde Custom Grade), containing a trace amount of Ar, and nitrogen-15 (98+%, Monsanto) were purified by Supelco high capacity carrier gas purifiers. The trace argon acted as an internal time base for the transient switches, defining the holdup in the gas phase.

Catalysts

The Haldor Topsøe KMIR, a prereduced triply promoted ($Al_2O_3/K_2O/CaO$) Fe catalyst, was employed in this study. The catalyst pellets (1.5–3 mm) were crushed and sieved for the −80/+100 mesh fraction. The BET surface area for the catalyst was determined to be 11.5 $m^2 \cdot g_{cat}^{-1}$. Two different admixtures of the catalyst pellets and inert glass beads (5-A Ferro Microbeads) of roughly the same mesh size were employed in the study—52 mg of KMIR diluted by 560 mg of glass beads and 106 mg of KMIR with 244 mg of glass beads. Each catalyst sample was activated prior to the reaction studies in the reactor by a stoichiometric flow of the purified H_2/N_2 mixture. The activation was conducted at 204 kPa total pressure and a space velocity of about 132,000 hr^{-1} according to the temperature program prescribed by the manufacturers (i.e., 300–523 K [5 hr], 523–653 K [7 hr], 653–748 K [10 hr], 723–748 K [5 hr]).

Reactor

The well-mixed reactor employed in the study facilitated the interpretation of the transient data (*3*). The reactor was constructed of 316 stainless steel with a copper gasket seal. A detailed description of the reactor and the proof for the uniformity of reactant concentrations, as seen by the catalyst, will be given elsewhere (*7*). The two different admixtures of KMIR and glass beads yielded steady-state and transient-kinetic ammonia synthesis data which suggested no significant heat transport effects. The apparent activation energies obtained on these catalyst samples which were reactant flow rate independent and in good agreement with literature values (*7*) permitted the conclusion that mass transport limitations did not affect the data reported here.

Procedure

The SSITKA experiments were performed at temperatures of 623 to 773 K, total pressures of 204 and 513 kPa, and ammonia synthesis conversion efficiencies, η ($P_{NH_3}/P_{NH_3,equilibrium}$), of 0.1 to 1.0. The ratio of H_2 to N_2 was 3 while the space velocities estimated at the reactor inlet were in the range 7400 to 74,000 hr^{-1}. With the catalyst well stabilized and reaction at steady-state for the conditions of each experimental run, a switch was made from a stoichiometric reactant feed of $^{14}N_2$ (trace Ar) and H_2 to one of $^{15}N_2$ and H_2 (Fig. 1). Back pressure regulators served to balance the pressure on the vent side of the zero dead volume switch valve (Valco) to that on the reactor side. This step ensured no pressure perturbations during the switch. The concentration of $^{14}NH_3$, $^{15}NH_3$, $^{14}N_2$, $^{14}N^{15}N$, $^{15}N_2$, and Ar (m/e = 17, 18, 28, 29, 30, and 40, respectively) were continuously monitored by an on-line quadrupole mass spectrometer (Extranuclear Model 2750-50) interfaced to a microcomputer for data logging. The reverse switch from $^{15}N_2$ to $^{14}N_2$ was also followed in the same manner. The constant level of ammonia production was verified by independent gas chromatographic analysis. A low electron excitation energy of 15 eV was employed for all mass spectrometric analyses thus ensuring negligible fragmentation of the primary labeled species. The mass spectrometer housing was kept at temperatures of 383–413 K to minimize NH_3 adsorption within the instrument.

The empty reactor, packed with the diluent glass beads, was conditioned in the manner described above for the catalyst ac-

tivation and was found to produce no ammonia under the reaction conditions used in this investigation. There was also no evidence for any dinitrogen activation in the absence of the catalyst (N-isotopes mixed to form $^{14}N^{15}N$ only in the presence of the catalyst as shown later). This glass-packed reactor was considered as the blank for the assessment of any extraneous contributions to the observed NH_3 transients. Synthetic mixtures of the same composition as those produced during the reaction runs were subjected to step NH_3 concentration changes. The switches were from (NH_3 + N_2 + H_2) to pure H_2 for the blank reactor.

The $^{14}N/^{15}N$ steady-state isotopic transient experiments described above permitted the tracing of the trajectory followed by nitrogen in the ammonia synthesis reaction pathway (N-path). A similar analysis was conducted for information on the H-path by switching from (H_2 + N_2) to (D_2 + N_2) and vice versa. This time NH_nD_{3-n} ($m/e = 20 - n$; $n = 0$, 1, 2, and 3), H_2, HD, and D_2 (m/e = 2, 3, and 4, respectively) were monitored. The degree and time dependence of the kinetic isotope effect on synthesis rates were established by the mass spectrometric signals for the NH_nD_{3-n} species. The signal linearity and mass invariance of the sensitivities of mass spectrometric signals due to the NH_nD_{3-n} species were verified by titration of the product mixture with a dilute standardized (0.01 *N*) HCl solution. The time required to completely neutralize a known volume of the acid solution by a constant flow of reactor effluent gave an independent measure of ammonia/deuteroammonia concentrations that were free from isotope effects. The H/D substitution experiment was repeated for the blank reactor through which was flowing a synthetic reaction mixture, containing NH_3 at a concentration approximately the same as that produced by the catalyst during the above H/D exchange experiment.

In order to gain more insight into the identity of the surface intermediates and to evaluate the influence of hydrogen in dinitrogen activation, isotopic switches were also made between $^{14}N_2$ and $^{15}N_2$ with He replacing H_2 in the reaction mixture. These latter experiments also provided estimates of available surface-exposed Fe. Prior to the N-isotope switches under He, a catalyst sample, which had been continuously under ammonia synthesis conditions for 21 days, was exposed to a flow of pure H_2 for 24 hr at 773 K. Before the introduction of N_2, the catalyst was conditioned for another 24 hr at 773 K under a flow of pure He. The latter step allowed for the complete desorption of hydrogen from the reactor walls and, perhaps, from the bulk phase of the catalyst. After the N_2 chemisorption experiments the catalyst was again reexposed to the synthesis gas. Subsequent replication of SSITKA on reaction at 673 K indicated that the catalyst had undergone no irreversible changes from the high temperature treatment. A more detailed discussion on the above nontraditional method of measuring N_2 chemisorption is given elsewhere (*12*).

RESULTS

When an abrupt switch was made from ($^{14}N_2$ + trace Ar + H_2) to ($^{15}N_2$ + H_2) over the lined-out KMIR catalyst at 723 K, 204 kPa, and efficiency, η, of 0.42, the transient curves shown in Fig. 2 were obtained. The net reaction rate and hence P_{NH_3} were not perturbed by the isotopic switch since ($^{14}NH_3$ + $^{15}NH_3$) remained constant throughout the experimental run.

Also shown in Fig. 2 is the NH_3 (blank) curve following a switch from (NH_3 + N_2 + H_2) to H_2 over a reactor packed with the diluent glass beads at the same temperature, pressure, and P_{NH_3} as the above steady-state transient run. The significant delay in the steady-state transient of $^{14}NH_3$ (KMIR), relative to the NH_3 (blank) curve, indicates that the former originates from catalyst-bound N-containing intermediates. The small lag between NH_3 (blank) and Ar appears to be of negligible consequence to the isotopic steady-state reaction transient

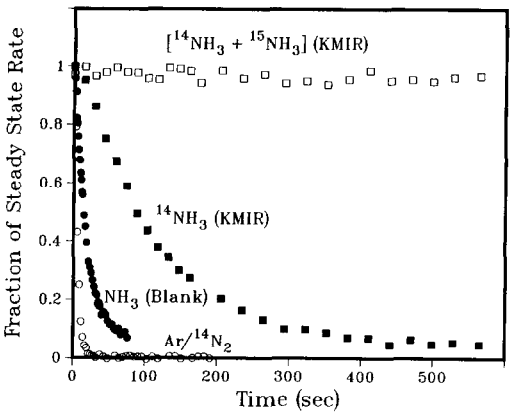

FIG. 2. Steady-state transients for $^{14}NH_3$, ($^{14}NH_3$ + $^{15}NH_3$), and Ar and $^{14}N_2$ (overlaying each other) due to a switch from ($^{14}N_2$ + Ar + $3H_2$) to ($^{15}N_2$ + H_2) over KMIR (run No. 11.5) versus a step NH_3 switch over the blank reactor showing the origin of $^{14}NH_3$ as catalyst-bound N-intermediates.

of $^{14}NH_3$ since the resulting lineshape for the latter shows no contribution to the mean relaxation time from decay processes having time scales comparable to that of the NH_3 (blank) transient. The lag in the blank experiment, which showed virtually no dependence on the reactor temperature or pressure at the conditions of this study, was probably due to an experimental artifact unimportant in the steady-state transient runs—for example, NH_3 adsorption in the small unheated dead volume between the shutoff valve on the (NH_3 + N_2) and H_2 lines before the reactor.

The NH_3 (KMIR) isotopic transient curves, as explained later, suggest *a single main pool of N-intermediates* as opposed to multiple reservoirs of surface intermediates in series. Figures 3a and 3b are typical steady-state transient curves for labeled NH_3 obtained after the indicated durations of exposure of the catalyst sample to the nitrogen isotopes. The virtual coincidence of these curves indicates the absence of kinetic isotope effects in the intrinsic catalytic processes on the catalyst surface and the absence of significant contributions to the rate by nitrogen from the bulk metal phase. Figure 4 shows data obtained at different temperatures while maintaining all reactant partial pressures essentially constant (P_{NH_3} varied from 309 to 488 Pa). Table 1 provides more detailed information about each run shown in Figs. 2–4.

With the exception of data taken at 773 K, there was no evidence for the desorption of mixed nitrogen ($^{14}N^{15}N$) during the synthesis reaction. At 773 K, as illustrated by Fig. 5a, N-isotope scrambling was observed. Figure 5b shows typical desorption curves for mixed nitrogen under hydrogen-free atmospheres. At temperatures of 723 K

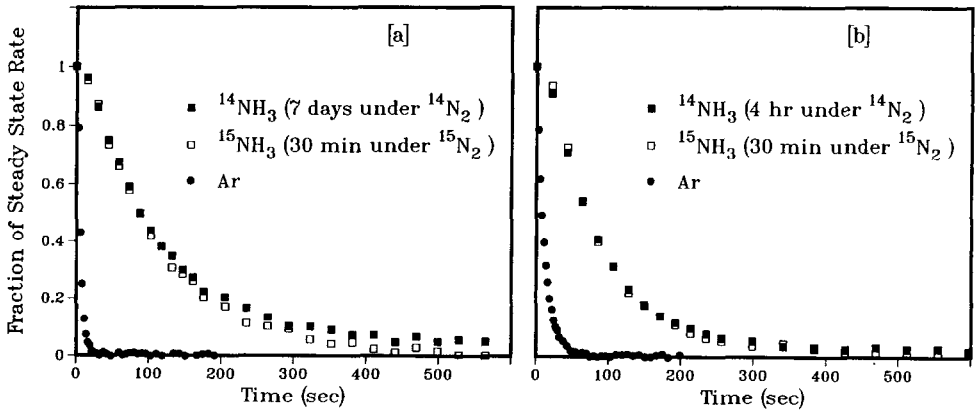

FIG. 3. Steady-state transients obtained after various durations of exposure to N-isotopes under reaction conditions at 723 K during [a] run No. 11.5 and its reverse isotope switch, and [b] run No. 12.1 and its reverse.

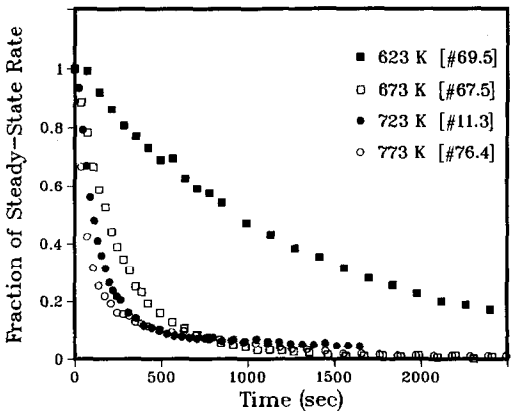

FIG. 4. $^{14}NH_3$ transient curves at different reaction temperatures with all reactant partial pressures held approximately constant.

and lower, $^{14}N^{15}N$ formation was observed only in the absence of hydrogen and in the presence of the catalyst, but its formation rate was extremely slow. It is well known (*4*) that the ammonia synthesis reaction, which entails the dissociation of dinitrogen, takes place readily even at 623 K (see Fig. 4) and lower over Fe-based catalysts. The blank reactor showed no N-isotope scrambling whatsoever, at the above conditions. Table 2 summarizes the nitrogen adorption data.

Figure 6 shows the nitrogen adsorption isotherm derived by integrating the transient curves such as those shown in Fig. 5. Following a step switch from one N-isotope to the other, catalyst-bound N-species desorbed mainly as $^{14}N^{15}N$. Desorption as $^{14}N_2$ or as $^{15}N_2$ was considered negligible since the transient curves for these species were essentially coincident with the curves observed for inert tracers. A small time lag between Ar and $^{14}N_2$ at high pressures was found to be entirely attributable to diffusional control of flow through the capillary tubing that connected the mass spectrome-

TABLE 2

Nitrogen Adsorption at 773 K under (He + N_2)[a]

Run No.	P (kPa)	P_{N_2} (kPa)	N_{ads} (μmol · g_{cat}^{-1})
77.5	204	13	21.1
77.6	204	13	20.0
78.1	204	25	27.8
78.2	204	25	25.7
78.6	204	51	76.0
79.1	204	51	81.5
76.5[a]	204	51	77.6[b]
79.2	307	82	148.4
79.3	307	82	121.8
79.4	513	130	128.0
79.5	513	130	147.7

[a] Run No. 76.5 was under (H_2 + N_2).
[b] N-intermediates leaving surface both as NH_3 and as $^{14}N^{15}N$.

TABLE 1

Coverage in Nitrogen-Containing Intermediates

Run No.	T (K)	P (kPa)	P_{NH_3} (Pa)	η	Coverage[b] (μmol · g_{cat}^{-1})	θ[a]
			Effect of total pressure			
11.5	723	204	234	0.42	80 ± 15	0.41
12.1	723	513	1060	0.23	108 ± 10	0.56
			Effect of reaction temperature			
69.5	623	204	392	0.11	120	0.63
67.5	673	204	426	0.26	141	0.73
11.3	723	204	309	0.61	100	0.52
76.4	773	204	488	1.0	19.2	0.10

[a] Based on the BET surface area of 11.5 m_2 · g_{cat}^{-1} and 10^{19} Fe atoms · m^{-2}.
[b] N-intermediates leaving surface as NH_3.

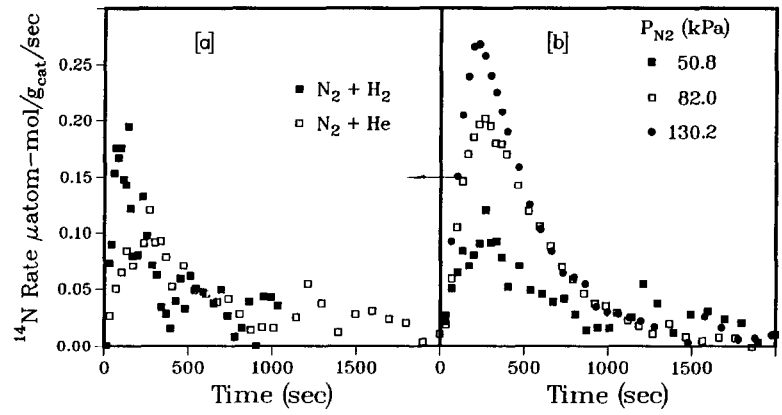

FIG. 5. Rate of desorption of surface N-atoms as $^{14}N^{15}N$ (in μatom mol of $^{14}N/g_{cat}$/sec) following typical switches from $^{14}N_2$ to $^{15}N_2$ at 773 K [a] in the presence (■) or absence (□) of H_2 at P_{N_2} = 51 kPa; [b] at various P_{N_2} under (N_2 + He).

ter to the reactor exit (*12*). It was however much smaller than the holdup times of the mixed nitrogen ($^{14}N^{15}N$) and did not affect the estimation of coverages, made above, for strongly adsorbed nitrogen. It may therefore be concluded that nitrogen was not present in significant amounts on the surface at these conditions as $*N_2$. Also indicated in Fig. 6 is the total N-coverage under ammonia synthesis conditions at 773 K during run No. 76.5. For the SSITKA data taken at the lower temperatures, the $^{14}N_2$ transient curves coincided with the Ar curve and $^{14}N^{15}N$ was present only at a concentration level corresponding to the 0.4% natural abundance of ^{15}N in nitrogen. The coincidence of the Ar and nitrogen transient curves suggests that the coverage in any weakly chemisorbed nitrogen must also have been negligibly small at the lower reaction temperatures.

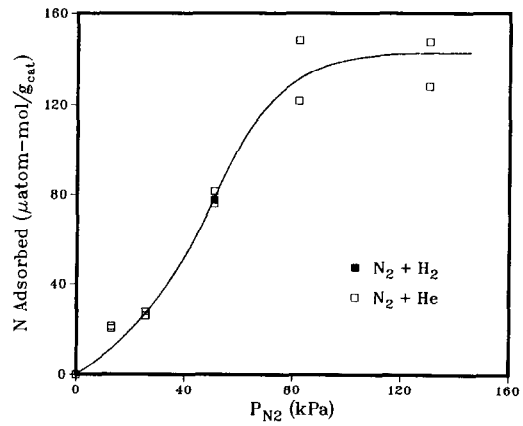

FIG. 6. Nitrogen adsorption isotherm at 773 K from transient experiments listed in Table 2.

The N-intermediates inventory of the working catalyst was computed from the product of the steady-state synthesis rate (mol · g_{cat}^{-1} sec^{-1}) and the area (sec) between the steady-state NH_3 transients and the Ar curve (the latter defining the gas phase holdup). Table 1 gives the coverages in nitrogen-containing intermediates at the conditions of this work.

The isotopic transient curves due to a switch from (N_2 + H_2) to (N_2 + D_2) are presented in Fig. 7. The solid curves of Fig. 7 represent the relaxation and growth curves expected if hydrogen and deuterium were statistically distributed in gas phase hydrogen and ammonia, respectively. Such statistical distribution signals the rapid rate of the adsorption/desorption steps involving these reactants. Figure 8 illustrates the evolution of the kinetic isotope effect on the steady-state rate of NH_3 synthesis. The data of Fig. 7 are replotted in Fig. 9 to show the net relaxation of hydrogen leaving the reactor as H_nD_{2-n} (F_H) or as NH_nD_{3-n}

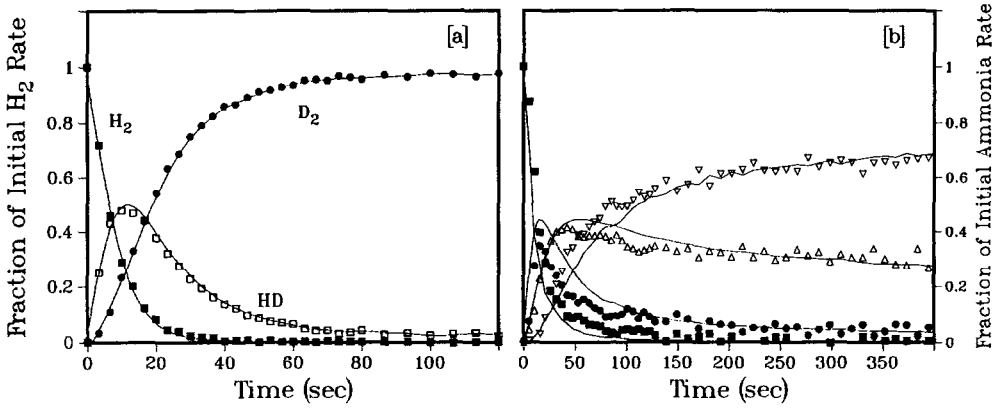

FIG. 7. Isotopic transients following a switch at 513 kPa and 723 K from ($3H_2 + N_2$) to ($3D_2 + N_2$): [a] H_2 (■), HD (□), and D_2 (●); [b] NH_3 (■), NH_2D (●), NHD_2 (△), and ND_3(▽). Solid curves are those expected if hydrogen is statistically distributed in H_nD_{2-n} and NH_nD_{3-n} [reaction conditions are those of run No. 12.1].

(F_{HA}) at the conditions of run No. 12.1. Figure 9 also displays the same information (F_D and F_{DA}, respectively) for deuterium upon a switch from ($N_2 + D_2$) to ($N_2 + H_2$).

The H and D (ex-H_nD_{2-n}) holdups in the reaction system were determined in the above experiment and its reverse isotope switch to be 15,430 and 4282 μatom-mol · g_{cat}^{-1}, respectively. This reveals that the hydrogen (deuterium) uptake could not all have come from the catalyst alone. This follows from comparisons with uptakes expected of the catalyst, assuming equilibrium dissolution of hydrogen in the bulk of the catalyst, where it is taken to be α-Fe (*13*). From the F_{HA} and F_{DA} curves, the holdups in H and D were estimated to be 1509 and 433 μatom-mol · g_{cat}^{-1}, respectively. Hydrogen/deuterium isotope switches over the empty reactor gave data which are not significantly different from

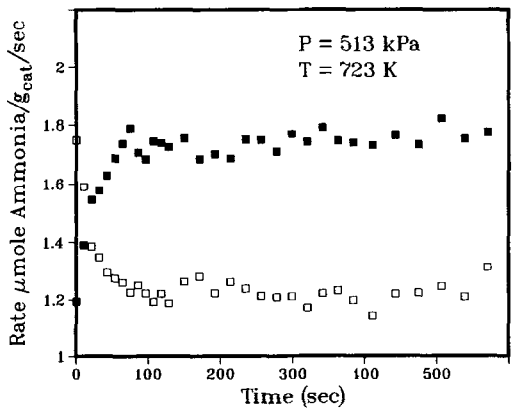

FIG. 8. Response curves for the total NH_nD_{3-n} production rates at 513 kPa and 723 K following a H_2-to-D_2 switch (■) and the reverse D_2-to-H_2 switch (□) [reaction conditions are those of run No. 12.1].

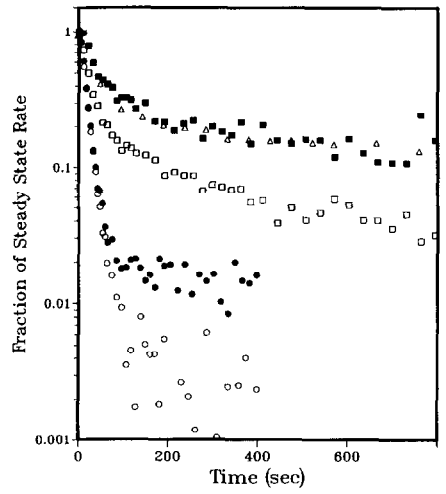

FIG. 9. Response curves at 513 kPa and 723 K for H in H_nD_{2-n} (●) and H in NH_nD_{3-n} (■) following a H_2-to-D_2 switch and for D in H_nD_{2-n} (○) and D in NH_nD_{3-n} (□) following a D_2-to-H_2 switch [from Figs. 7 and 8], compared with response of H in NH_nD_{3-n} (△) for a H_2-to-D_2 switch over a blank reactor using a synthetic product mixture at the same conditions.

those over the catalyst. This point is illustrated in Fig. 9 by the F_{HA} curves corresponding to the two cases. The corresponding F_H and F_D responses were virtually coincident with each other and with the curve expected of an inert tracer, but for the slowly decaying tails. In the blank run, a gas mixture of the same composition as that produced during the synthesis reaction was flowing through the reactor. The slight lag between the two F_{HA} response curves (the one obtained under reaction conditions over the catalyst and the other derived from H/D exchange over the blank reactor under the flow of a synthetic product mixture) corresponds to a holdup of about 30 μatom-mol $\cdot$ g_{cat}^{-1} of H which leaves the reactor as NH_nD_{3-n}. This estimate is, however, of the same order of magnitude as the error of determining the H-intermediates content from F_{HA} and as such does not provide a reliable measure of hydrogen coverage.

The reactor is responsible for most of the observed hydrogen holdup. In view of the relatively small internal surface area of the reactor (about a tenth as large as the net BET surface area of the catalyst) and the large time constant of the tails to the hydrogen transient curves, it may be concluded that the bulk phase of the reactor walls accounts for a significant part of the hydrogen retention. Concerns that there may also be a reactor wall contribution to the N-intermediate coverage were addressed earlier and are further allayed by the significant temperature dependence of the nitrogen holdup curves and coverages (see Fig. 4 and Table 1). The hydrogen holdups are much less sensitive to temperature variations. Moreover, SSITKA data on Ru-based catalysts (*12*) in the same reaction vessel show much lower nitrogen holdups than those observed here at comparable reaction conditions on the iron catalyst.

DISCUSSION

Coverage by Intermediates

Very few quantitative determinations have been made in the past of the coverage in N-intermediates on ammonia synthesis catalysts under reaction conditions. Scholten *et al.* (*14*) reported fractional coverages of 0.44 to 0.54 for N-intermediates on doubly promoted (Al_2O_3/K_2O) Fe catalysts based on microgravimetric measurements. The study of Boreskova *et al.* (*15*) implied a N-coverage of 0.28 for their triply promoted ($Al_2O_3/K_2O/CaO$) Fe catalyst at 573 K, 101 kPa, and H_2/N_2 of 10. Ertl and co-workers (*16*), on the other hand, obtained somewhat lower N-coverages (0.07 at 583 K, 81 kPa, and $H_2/N_2 = 3$) on an Fe(111) single crystal surface by means of *ex situ* Auger electron spectroscopic analysis of the sample after evacuating the gas phase reactants at the temperature of reaction. While the present results for coverage by N-intermediates (0.1–0.73) show fairly good agreement with the *in situ* measurements of Scholten *et al.*, the data presented here represent truly reactive surface intermediates (as opposed to dormant surface or bulk species). The N-intermediates coverage data were determined at the conditions of steady-state reaction. The recent quantum mechanical calculations by Stoltze and Nørskov (*17*) also suggest high N-intermediates coverage. Their model extrapolated, to practical reaction conditions, the UHV data of Ertl and co-workers (*16*).

It is generally believed that the surface of the working ammonia synthesis catalyst is covered predominantly by N-containing reaction intermediates (*4*, *17*). Consequently, the catalyst coverage in adsorbed atomic hydrogen (*H) is assumed negligible during the synthesis reaction. Within the limits of the error in determining H-intermediates coverage in this study, it may be concluded that hydrogen holdup (both as *H and in $*NH_x$) on the catalyst is much smaller than the N-coverage. However, in a recent *in situ* Raman spectroscopic analysis of the reaction on a triply promoted iron catalyst, Zhang and Schrader (*18*) concluded that *H and $*N_2$ are the main intermediates at 673 K. If the ease of migration in and out of the reactor walls observed in the present study

is anything to go by, one may expect a considerable part of the hydrogen inventory of the working catalyst to come from bulk-phase contributions. If the bulk phase of the Fe component of the catalyst sample employed in the H/D exchange experiment was saturated by H-species, the resulting H-intermediates content would be about 50 μatom-mol $\cdot$ g_{cat}^{-1} compared to approximately 140 μatom-mol $\cdot$ g_{cat}^{-1} (see Fig. 6) required to saturate the catalyst surface. A significant migration of hydrogen in and out of the bulk phase of Fe single crystals has been reported by Cavalier and Chornet at room temperature and UHV pressures (*19*). Furthermore, the high coverage in N-intermediates observed here (Table 1) and suggested elsewhere (*17*) implies a low surface occupancy by hydrogen which is unassociated with N-species. Stoltze and Nørskov (*17*) estimated θ_{*H} to be of the order of 10^{-3} compared to a θ_{*N} of 0.5 or greater at 10 MPa and 673 K.

The dissolution of hydrogen species into the bulk phase of the catalyst as suspected above leads to the question of the possible participation of bulk-phase nitrogen in the steady-state reaction. There have also been reports, in the literature, of the bulk dissolution of nitrogen in triply promoted iron catalysts during ammonia synthesis (*20, 21*). Silveston and co-workers (*20*), for instance, found a substantial amount of bulk nitrogen from non-steady-state (step N_2 concentration switch) transient analyses. The present study suggests that such bulk N-species are insignificant participants in the steady-state reaction. This conclusion comes from the absence of any significant dependence of the steady-state transient curves of Figs. 3a and 3b on durations of exposure to N-isotopes and the absence of slowly decaying tails in the N-isotope response curves of Figs. 2–5. The transients observed by Silveston *et al.* show a notable "tail-section" compared to these curves.

Data of non-steady-state transient experiments in our laboratory, the details of which will be discussed elsewhere (*12*), corroborate the results of Silveston's group. A depopulation of the surface in N-intermediates in the course of such non-steady-state transients perhaps encourages the slow migration of bulk N-species to the surface followed by their subsequent hydrogenation. The conclusion is that bulk-phase nitrogen (if present) remains, essentially, a fixed part of the catalyst matrix under steady-state reaction conditions. Such nonparticipating species may erroneously show up as intermediates in nondiscriminating analytical methods. As will be seen later during the discussion of surface heterogeneity, the initiation of a significant contribution to the steady-state reaction from a second less reactive N-intermediate pool only occurred for temperatures of at least 723 K, way above the 673 K employed in the Waterloo study (*20*).

The $^{14}N_2/^{15}N_2$ switches over the catalyst in the absence of hydrogen also yielded results which are germane to the debate of bulk-N participation in the steady-state reaction. No tails of the type observed for the H/D transient curves were evident in the nitrogen curves (see Fig. 5). From the nitrogen adsorption isotherm of Fig. 6 and the (11.5 $m^2 \cdot g_{cat}^{-1}$) BET surface area of the catalyst, it may be inferred that 73% of the working catalyst surface was active in nitrogen adsorption (assuming 10^{19} Fe atoms/m^2). Thus, the Fe content of the surface is high even though a substantial segregation of the promoters to the surface has been reported in the literature (*16, 21*).

Mechanism

Conclusions, from this study, on the path traced by hydrogen in the ammonia synthesis reaction must be drawn with caution in view of the large contribution to the hydrogen transients from the reactor walls. Even so, it may be inferred that the adsorption–desorption steps involving both H_2 and NH_3 are fast and essentially equilibrated. This follows from Fig. 7 which shows rapid scrambling for H and D in these species. The low coverage in the H-intermediates on

the catalyst also underscores the rapid rates of these elementary steps. This is in agreement with the literature view on the relative rates of these steps (*4, 22*).

Similar considerations regarding the N-path present a somewhat different picture. It can be inferred that a kinetically significant step exists on the N-path between the dinitrogen adsorption step and the main N-containing surface intermediate. This follows from the lack of observable isotopic mixing of ^{14}N and ^{15}N (except in the absence of H_2), the significant time lag between the transient response of $^{14}N_2$ and that of $^{14}NH_3$, and the absence of any lags (under reaction conditions) between the Ar curves and the $^{14}N_2$ and $^{14}N^{15}N$ responses. This is consonant with the generally held view in the literature (*4, 21, 23*) that dinitrogen dissociation is rate determining and that the most abundant surface N-intermediate is not equilibrated with gas phase N_2. The transient curves of Figs. 2–4 imply one main pool of N-intermediates since the characteristic sigmoid shape expected of multiple pools of surface intermediates in series (*24*) is not evident in these curves. The slight hints at the sigmoid shape in some of the isotopic NH_3 transient line shapes were absent when the curves were corrected for gas phase holdup (*12*). Furthermore, it can be shown (*12*) that two or more irreversible (kinetically significant) elementary steps are required on the N-path to generate a system of multiple pools of N-intermediates in series. Thus, the data of the present study suggest a single rate-limiting step involving nitrogen.

By comparing the $^{14}N^{15}N$ transients of Fig. 5 (with and without H_2) and the relative ease of isotopic transfer of N to ammonia at the lower reaction temperatures (Fig. 4) it may be inferred that N_2 dissociation is enhanced by hydrogen. However, in the presence of H_2 the preferred exit channel for the N-intermediates is $NH_3(g)$ rather than $N_2(g)$. Perhaps the provision of this alternate exit channel, which might entail a relatively "cleaner" active surface, is responsible for the enhancement of N_2 activation. This will be particularly true if hydrogen does not strongly compete for the active sites so regenerated.

The foregoing presumes that the identity of the N-intermediates under a hydrogen-free atmosphere is the same as that stable under ammonia synthesis conditions. While this may not exactly be the case, the generally accepted view of negligible coverage in surface *H reduce the uncertainty in the identity of the most abundant reactive intermediate (MARI) to these possible candidates: $*NH_x$ and $*N_2H_x$. Clearly in the absence of H_2, *N is the predominant surface species as indicated by the data of Fig. 5 which show that nitrogen is not held on the surface as $*N_2$ at 773 K. On the basis of Fig. 5a, it may be suggested that the surface was not significantly modified by the withdrawal of H_2 and that the N-intermediate in the two cases is stoichiometrically identical based on the closely similar N-isotope scrambling curves of this figure. On the basis of the above reasoning it is suggested that x is ca. 0 and that the MARI contains nitrogen in the dissociated atomic state.

Assuming *N to be the MARI, then the "surface-cleaning" hypothesis is not supported by the N_2 coverage data of Fig. 6 and Table 2 which, at P_{N_2} and temperature conditions of run No. 76.5, suggest virtually the same N-coverage with or without H_2 present in the reactant mixture. An alternate explanation of the hydrogen enhancement of dinitrogen activation is direct hydrogen-assisted dissociation of the N≡N bond through the predissociation formation of an N_2H_z complex, as was proposed by Temkin and Pyzhev (*25*) and more recently by Zhang and Schrader (*18*). It is, however, unlikely that such a complex would constitute the MARI, as implied by the latter authors, if the cleavage of the N≡N remains a kinetically significant step with $NH_3(g)$ equilibrated with the surface intermediates and if, as argued above, x is zero. If it exists, the complex is probably in rapid equilibrium with the gas phase N_2 and H_2 but

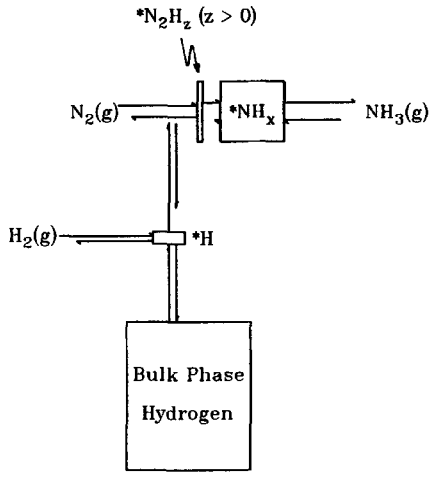

FIG. 10. Schematic of the suggested mechanism for ammonia synthesis over KMIR.

represents a minor surface intermediate, hence the absence of a significant sigmoid character in the isotopic NH_3 transient curves. There has been spectroscopic evidence for an $*N_2H^+$ species from the field emission experiments of Schmidt (*26*) on iron.

In view of the foregoing and the virtual equilibration of the adsorption–desorption steps involving $NH_3(g)$ and H_2, we propose that hydrogen facilitation of dinitrogen dissociation proceeds via an $*N_2H_z$ complex which itself is a minor surface species.

The above suggestions about the reaction mechanism are summarized schematically in Fig. 10. The lengths of the arrows of the figure are intended to reflect the relative rates of the elementary reaction (or adsorption–desorption) steps (*1*), while the sizes of the boxes enclosing the intermediates reflect the relative abundances.

Kinetic Manifestation of Surface Heterogeneity

The necessity for explicit accounting of surface nonuniformity in practical catalysts in the formulation of ammonia synthesis rate expressions, as was accomplished by Temkin and Pyzhev (*25*), has often been questioned (*17, 27–29*). The resulting rate expressions do not, in any case, differ significantly from those employing the more convenient Langmuirian assumptions (*5, 17, 28, 30*). Justification for formulations of the Temkin–Pyzhev type come from observations of coverage dependency in the heats of chemisorption over ammonia synthesis catalyst (*25*). Ertl (*16*) has suggested that one role of the K_2O promoter in practical catalysts is to annul the activity variations over the surface. It should be noted, however, that these catalysts still display a coverage-dependent heat of adsorption as was illustrated by Topsøe *et al.* (*31*) for CO chemisorption over KMIR.

Since the working catalyst as implied by the absence of sigmoidal-shaped transient response curves (Figs. 2–4) does not contain more than one observable pool of N-intermediates in series, a linear curve would be expected of the semilogarithmic representation of the steady-state NH_3 transient data if the surface were kinetically uniform, i.e., if the lifetimes (τ) in the single intermediates pool were the same for all the intermediate molecules (atoms) (*8*). A distribution of lifetimes characterizes nonuniform surfaces and would be reflected in an upward concavity of the semilogarithmic curves. Figure 11 shows that the working catalyst exhibited kinetic heterogeneity at the conditions of this study except at 623 K.

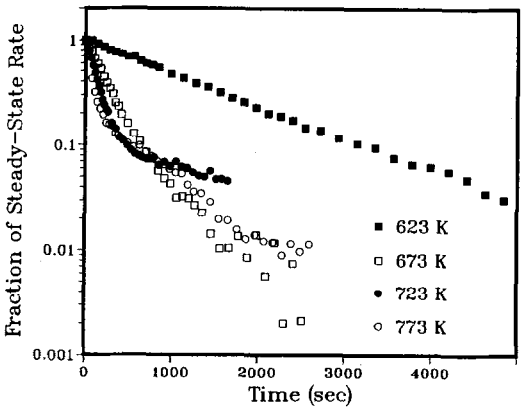

FIG. 11. Semilog plot of the $^{14}NH_3$ transients of Fig. 4.

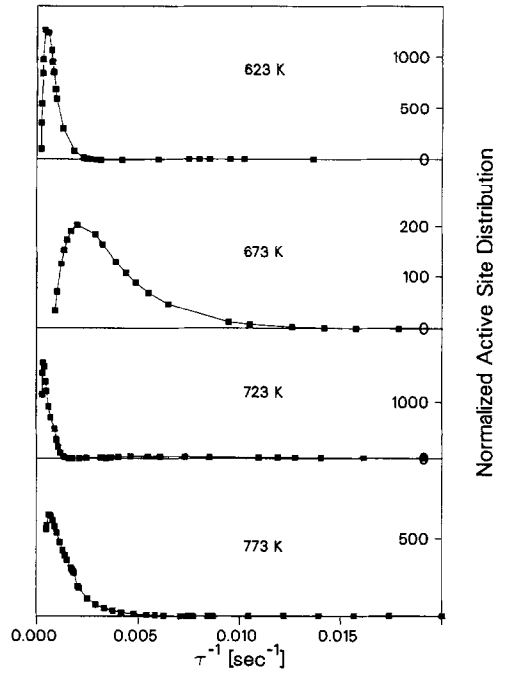

FIG. 12. Active-site distribution over the working catalyst (from data of Fig. 4).

Figure 12 illustrates a deconvolution of the $^{14}NH_3$ response curves, in terms of activity distributions over the catalyst surface using the Laplace inversion method recently introduced by De Pontes *et al.* (*8*). A more detailed discussion of these *a priori* distribution curves will be given along with a presentation of the kinetic interpretation of the curves based on the model of Temkin and Pyzhev in a separate communication (*32*). As the temperature was raised from 623 to 773 K, with the reactant partial pressures maintained essentially constant, an interesting trend developed in the activity distribution. As the temperature was raised from 623 to 673 K, the breadth of the distribution increased and the mean lifetime shifted to a lower value. This should be expected since lifetimes derived from SSITKA are measures of the intrinsic turnover frequency of the surface (*24*). This trend would appear to have been reversed between 673 and 723 K. What actually happened was, however, that a second less reactive pool developed at the higher temperatures, dwarfing the more active pool which is related to the low temperature pools. Figure 13 shows a magnification of the high activity end of the site distribution scale and indicates the percentage contributions to the total reaction rate from these peaks. At 723 and 773 K these higher activity sites, accounting for only 10% of the total active site density, contributed 73 and 89%, respectively, to the net steady-state ammonia production. Barring a restructuring of the surface, the new less reactive pool may have arisen from previously dormant or saturated active sites. There is also the possibility that the hitherto unimportant bulk-phase nitrogen was now a participant in the reaction at the elevated temperatures. The active-site distribution curves are additional indicators of the extent of kinetic heterogeneity of the working surface.

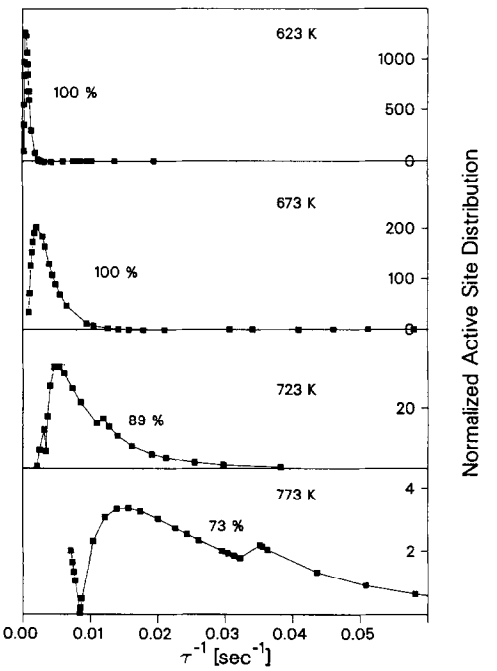

FIG. 13. Effect of temperature on the activity distribution in the main N-intermediates pool (from data of Fig. 4).

CONCLUSIONS

This study has yielded the first direct, measurements under steady-state reaction conditions, of the coverages of a working ammonia synthesis catalyst in nitrogen-containing intermediates. It also provides an assessment of the hydrogen coverage and its possible participation in the rate-limiting step. The most abundant reaction intermediate is suggested to be *N. It was concluded that bulk-phase nitrogen species do not participate significantly in the steady-state reaction as intermediates at temperatures of 673 K and lower. The line shapes of the transient data of this study led to the inference that a single rate-limiting step exists in the synthesis pathway involving nitrogen. It would also appear that hydrogen facilitates this step which involves dinitrogen dissociation. The working catalyst surface was found to be kinetically nonuniform at the steady-state reaction conditions employed here, especially above 623 K.

ACKNOWLEDGMENTS

We gratefully acknowledge support for this work by the National Science Foundation (Contract NSF-CBT-8612229). One of us (J.U.N.) would like to thank the United States Information Agency for a Fulbright Junior Fellowship. We are also grateful to Dr. L. Galya who conducted the BET analysis of our catalyst sample.

REFERENCES

1. Tamaru, K., *in* "Advances in Catalysis" (D. D. Eley, W. G. Frankenburg, V. I. Komarewsky, and P. B. Weisz, Eds.), Vol. 15, p. 65 Academic Press, New York, 1964; "Dynamic Heterogeneous Catalysis." Academic Press, New York, 1978.
2. Yang, C.-H., Soong, Y., and Biloen, P., *in* Proceedings, 8th International Congress on Catalysis, Berlin, 1984." Dechema, Frankfurt-am-Main, 1984, Vol. II, pp. 3–14.
3. Happel, J., "Isotopic Assessment of Heterogeneous Catalysis." Academic Press, New York, 1986.
4. Boudart, M., *Catal. Rev. Sci. Eng.* **23,** 1 (1981).
5. Boudart, M., and Djéga-Mariadassou, G., "Kinetics of Heterogeneous Catalytic Reactions." Princeton Univ. Press, Princeton, NJ, 1984.
6. Krishna, K., M.S. thesis, University of Pittsburgh, 1985.
7. Nwalor, J. U., Krishna, K., Potter, M., Biloen, P., and Goodwin, J. G., Jr., manuscript in preparation.
8. De Pontes, M., Yokomizo, G. H., and Bell, A. T., *J. Catal.* **104,** 147 (1987).
9. Soong, Y., Krishna, K., and Biloen, P., *J. Catal.* **97,** 330 (1986).
10. Happel, J., Otarod, M., Ozawa, S., Yin, F., Chew, M., and Chen, H. Y., *J. Catal.* **84,** 156 (1983).
11. Bennett, C. O., and Tau, L. M., *J. Catal.* **89,** 327 (1984).
12. Nwalor, J. U., Ph.D. dissertation, University of Pittsburgh, 1988.
13. Hansen, M., "Constitution of Binary Alloys." McGraw–Hill, New York, 1958.
14. Scholten, J. J. E., Zwietering, P., Kovalinka, J. A., and de Boer, J. H., *Trans. Faraday Soc.* **55,** 2166 (1959).
15. Boreskova, E. G., Kuchaev, V. L., and Temkin, M. I., *Kinet. Katal.* **25**(1), 112 (1984).
16. Ertl, G., *Catal. Rev. Sci. Eng.* **21,** 201 (1980).
17. Stoltze, P., and Nørskov, J. K., *Phys. Rev. Lett.* **55,** 2502 (1985); *J. Catal.* **110,** 1 (1988).
18. Zhang, H.-B., and Schrader, G. L., *J. Catal.* **99,** 461 (1986).
19. Cavalier, J. C., and Chornet, E., *Surf. Sci.* **60,** 125 (1976).
20. Jain, A. K., Hudgins, R. R., and Silveston, P., *Canad. J. Chem. Eng.* **60,** 809 (1982).
21. Emmett, P. H., *in* "The Physical Basis of Heterogeneous Catalysis" (E. Drauglis and R. I. Jaffee, Eds.), p. 3. Plenum, New York, 1975.
22. Taylor, H. S., and Jungers, J. C., *J. Amer. Chem. Soc.* **57,** 660 (1935).
23. Ozaki, A., and Aika, K., *in* "Catalysis—Science and Technology" (J. R. Anderson and M. Boudart, Eds.), Vol. 1, p. 87. Springer, Berlin, 1981.
24. Biloen, P., *J. Mol. Catal.* **21,** 17 (1983).
25. Temkin, M. I., and Pyzhev, V., *Acta Phys. U.R.S.S.* **12,** 327 (1940).
26. Cited by Nielsen, A., *in* "An Investigation on Promoted Iron Catalysts for the Synthesis of Ammonia," 3rd ed. Gjellerups, Copenhagen, 1968.
27. Ozaki, A., Taylor, H., and Boudart, M., *Proc. R. Soc. A* **258,** 47 (1960).
28. Boudart, M., *AIChE J.* **2**(1), 63 (1956).
29. Rayment, T., Schlogl, R., and Thomas, J. M., *Nature (London)* **315,** 311 (1985).
30. Bowker, M., Parker, J. B., and Waugh, K. C., *Appl. Catal.* **14,** 101 (1985).
31. Topsøe, H., Topsøe, N., Bohlboro, H., and Dumesic, J. A., *in* Proceedings, 7th International Congress on Catalysis, Tokyo, 1980" (T. Seiyama and K. Tanabe, Eds.). Elsevier, Amsterdam, 1981.
32. Nwalor, J. U., and Goodwin, J. G., Jr., manuscript in preparation.